

Article

# Effect of N<sub>2</sub> Replacement by CO<sub>2</sub> in Coaxial-Flow on the Combustion and Emission of a Diffusion Flame

Haisheng Zhen \* , Zhilong Wei and Zhenbin Chen

The Mechanical and Electrical Engineering College, Hainan University, Haikou 570228, China; zhilongwei.xjtu@gmail.com (Z.W.); 13637690766@163.com (Z.C.)

\* Correspondence: ban18@126.com; Tel.: +86-898-6626-7576; Fax: +86-898-6626-7576

Received: 25 March 2018; Accepted: 19 April 2018; Published: 24 April 2018



**Abstract:** In this study, a double concentric burner burning methane with an annular coaxially-flowing oxidizer was adopted to operate the diffusion flame in lifted flame regime. The effects of coaxial-flow velocity, coaxial-flow composition variation through total and partial replacement of N<sub>2</sub>, and coaxial-flow oxygen enrichment were experimentally investigated in terms of the resultant changes in the flame stability, and thermal and emission characteristics. Consistent with the triple flame theory, the current stability tests show a linear increase in flame lift height with increasing coaxial-flow velocity and the blowout of lifted flames occurred at constant flame tip height. Replacement of N<sub>2</sub> by CO<sub>2</sub> in the coaxial-flow deteriorated the flame stability by significantly reducing the threshold coaxial-flow velocity. Due to combustion enhancement that is caused by oxygen enrichment, the threshold coaxial-flow velocity increased and this increase is more significant for the N<sub>2</sub>-diluted flame than CO<sub>2</sub>-diluted. Two of the most important NO<sub>x</sub> formation mechanisms, Zeldovich and Fenimore, were analyzed under the relatively low temperature flame conditions, generally below 1300 °C in this study. Results show that NO<sub>x</sub> is principally produced via the Fenimore mechanism for both N<sub>2</sub>- and CO<sub>2</sub>-diluted flames. NO<sub>x</sub> productions can be significantly affected by coaxial-flow composition and coaxial-flow velocity. An increase in the velocity of N<sub>2</sub>-diluted coaxial-flow increases NO<sub>x</sub> emissions, while a reverse trend occurred, as N<sub>2</sub> in the coaxial-flow was replaced or partially replaced by CO<sub>2</sub>, which is ascribed to the strong combustion-resisting behavior of CO<sub>2</sub>. For all cases, CO emissions vary in the opposite direction of NO<sub>x</sub> emissions. Due to the strong thermal and chemical effects of CO<sub>2</sub> on combustion in comparison to N<sub>2</sub>, total or partial replacement of N<sub>2</sub> by CO<sub>2</sub> results in a steep increase in CO emissions.

**Keywords:** flame stability; lift off height; coaxial-flow; dilution; CO/NO<sub>x</sub> emissions

## 1. Introduction

As the global demand of energy keeps surging, CO<sub>2</sub> discharge will further increase, thus leading to the anticipated worsened change in climate. Driven by public awareness and legislation for reducing CO<sub>2</sub> emission, oxy-fuel combustion coupled with flue gas recirculation (FGR) has been developed as a successful strategy in many combustion devices. Associating with it are many merits, including high CO<sub>2</sub> concentration in the flue gas as well as controlled flame temperature and pollutants emission [1]. The O<sub>2</sub>/CO<sub>2</sub> mixture has received prior interests of research due to its inherent relevancy to oxy-fuel combustion with FGR, and the fuels that are extensively investigated are coal and natural gas [2].

When CO<sub>2</sub> is used to replace N<sub>2</sub> in air, O<sub>2</sub>/CO<sub>2</sub> combustion occurs. It is anticipated that the flame structure, burning velocity, and air pollutants emission may be affected by the diluent present in the mixture. In the early 1980s, Horn and Steinberg [3] were the first to introduce the concept of O<sub>2</sub>/CO<sub>2</sub> combustion for coal combustion. Besides coal, previous researches were also conducted for O<sub>2</sub>/CO<sub>2</sub> combustion of natural gas. Exploring the chemistry mechanism of soot formation, Andersson

and Johnsson [4] reported that the situation of soot formation may be totally different for oxy-fuel combustion in comparison to air-fuel combustion. The reason is that the addition of CO<sub>2</sub> to pure O<sub>2</sub> increased the soot volume fraction and radiation heat transfer in the natural gas flames. Using calculations on a planar freely propagating flame, Liu et al. [5] numerically obtained the laminar burning velocity of O<sub>2</sub>/CO<sub>2</sub>/CH<sub>4</sub> mixtures at various equivalence ratios and pressures. The data showed that once the component N<sub>2</sub> in air was replaced by CO<sub>2</sub>, the laminar flame burning velocity was greatly reduced. Heil et al. [6] experimentally tested oxy-methane combustion on a 25 kW furnace, revealing that the existence of CO<sub>2</sub> has a significant influence on the production and consumption rates of CO. Working on an atmospheric pressure flow reactor for the oxy-fuel combustion of CH<sub>4</sub>, Glarborg and Bentzen [7] observed that the high CO<sub>2</sub> concentration leads to strongly increased CO emissions in the near-burner region. In the study of a flat flame, Watanabe et al. [8] discussed the effect of CO<sub>2</sub> reactivity on NO<sub>x</sub> formation and revealed that low NO<sub>x</sub> combustion can be achieved by varying CO<sub>2</sub> mole fraction in the inflow gas.

Lifted flames are preferred in certain combustion processes to protect the burner nozzle. To understand the basic stabilization of lifted flames, several theories arose to explain the characteristics of lifted flame. Phillips firstly observed a triple flame structure in a round turbulent jet flame [9]. Later on, many researchers explained the liftoff flame stabilization mechanism on this theory. For instance, Wu et al. [10] utilized the Rayleigh technique to image the distribution of fuel/air mixing levels in a turbulent diffusion jet flame. Instantaneous two-dimensional (2-D) mixing levels provide sound evidence to the existence of the triple flame structure. The triple or tribrachial structure also appeared in diffusion flame with co-flow. Lawn presented an extensive review of turbulent lifted flames in co-flowing air, summarizing that small increases in co-flow velocity lead to large increases in liftoff height, when compared to increases in jet velocity. In contrast to numerous studies on turbulent flames, studies on laminar flames are more recently conducted, including those of Lee et al. [11], Want et al. [12], and Jeon and Kim [13].

The literature review reveals that little previous attention was paid to the effects of CO<sub>2</sub> addition on flame stability characteristics. Even less work was done before on the partial replacement of N<sub>2</sub> by CO<sub>2</sub>. What is more important, previous studies on lifted flame paid much attention to the turbulent flame regime, while little work touched the laminar flame regime. Therefore, the present study is conducted to investigate the effects of N<sub>2</sub> replacement by CO<sub>2</sub> and oxygen enrichment on the flame stability. Moreover, the applicability of the popular stabilization mechanism for turbulent lifted flame, i.e., the triple flame theory, to laminar lifted flame is exploited. In order to better understand the laminar lifted flame behaviors, the effects of diluents of N<sub>2</sub> and CO<sub>2</sub>, or both of them, due to partial replacement would be compared in terms of the thermal and pollutants emission characteristics of the flames. The outcome of this work will provide guidance for better control of carbon dioxide emitted from practical combustors, in that the role of CO<sub>2</sub> needs to be distinguished concretely at varied conditions.

## 2. Experimental Setup and Method

The jet-in-coaxial-flow flames, where a central fuel jet issues into an outer coaxial-flow of oxidizer, are typically used for various combustors, and nearly all industrial flames are of this type. For current experimental study, a concentric double-port burner constructed by co-axially mounting two pipes of different diameters was utilized to operate the flames in laminar regime. The inner and outer pipes have 7 mm and 11 mm inner diameters, respectively, with 0.5 mm thickness. Laminar flows state was chosen because it is less touched on in previous researches.

Table 1 presents the flow conditions tested in this study. The fuel in the central nozzle is pure methane while the oxidizer, composed of pure oxygen and diluents of either nitrogen or carbon dioxide, or both, in the annular nozzle, co-axially flows with the central jet. All of the gases used are of purity of over 99.9% to avoid variation of composition, and calibrated flow meters were used to monitor and control the flow rates of supplied oxidizer and fuel. Following the convention of Ref. [14],

the concept of overall equivalence ratio, ' $\Phi$ ', which is evaluated based on the mass flow rate of the oxidizer and fuel in relation to the stoichiometric oxidizer and fuel ratio, was adopted in this study. Note that the secondary air that is entrained from ambient air into the flame is not considered into the concept of overall equivalence ratio.

**Table 1.** Range of flow conditions tested.

Oxygen Fraction	21%		24%		27%	
-	Range of volume flow rate ( $10^{-6} \text{ m}^3/\text{s}$ )	Mean flow velocity (m/s)	Range of volume flow rate ( $10^{-6} \text{ m}^3/\text{s}$ )	Mean flow velocity (m/s)	Range of volume flow rate ( $10^{-6} \text{ m}^3/\text{s}$ )	Mean flow velocity (m/s)
O <sub>2</sub>	0.2~13.9		0.3~12.8		0.8~39.0	
N <sub>2</sub> or CO <sub>2</sub>	0.9~52.5	0.02~1.18	0.9~40.6	0.02~0.94	0.3~14.4	0.02~0.94

Figure 1 schematically illustrates the experimental apparatus, which mainly consists of two parts: one part for flame thermal and stability characteristics testing and the other for air pollutants emission measurement. The concentric burner was enclosed by double layers of screen meshes for minimization of the disturbance from surrounding ambient air. The stainless steel meshes have a height of 300 mm and a hole size of 0.5 mm. The experiments were firstly performed by using a 21%O<sub>2</sub>–79%N<sub>2</sub> (by volume) mixture to mimic the situation of coaxial-flowing air reacting with central fuel. A high resolution CCD camera, operating at a shutter speed of 1/60s, was utilized to record flame images in a dark background. Luminous flames together with an adjacent parallel ruler were taken into photographs and then post-processing of the images was made to identify the flame height.

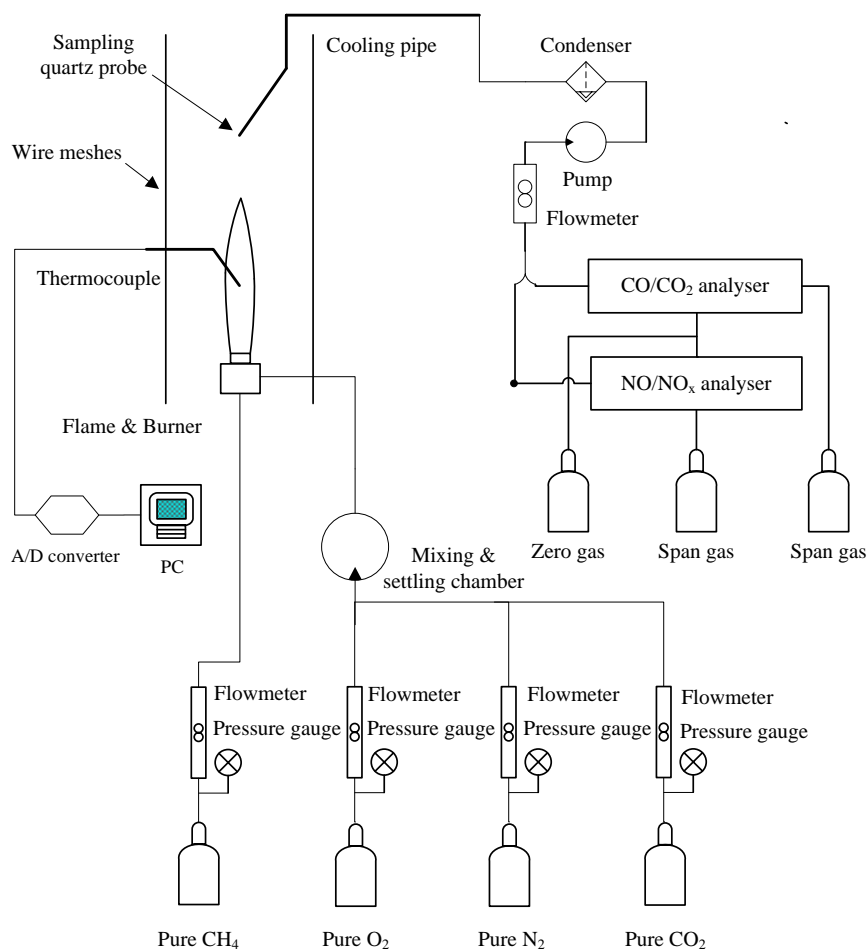


**Figure 1.** Sketch of the experimental apparatus.

Flame temperatures were registered by an uncoated type B thermocouple having a Pt-30%Rh anode and a Pt-6%Rh cathode. The wires have a diameter of 0.25 mm and their joint bead is smaller than 0.5 mm in diameter. Such sizes are small enough to reduce the error that is caused by thermal conduction, but big enough to keep the rigidity of the thermocouple. For each measurement, the thermocouple sampled 50 data successively within 10 s, and then the averaged value was corrected for radiation loss. As radiation loss is generally considered as an important source of error, all of the recorded temperatures were corrected according to the bare-bead thermocouple model of Blevins and Pittset al. [15]. The maximum correction is 44 °C at the directly measured temperature of 1306 °C in this study.

Secondly, flame stability phenomena, including attachment, liftoff, and blowout were experimentally tested by gradually increasing the oxidizer co-flow rate, while maintaining the fuel flow rate constant. Primary attention was paid to flame liftoff, and the dependence of lift height on the coaxial-flow mean velocity would be found out. Finally, the experiments were continued in two ways to allow for variations of the coaxial-flow composition. One is to replace N<sub>2</sub> in the coaxial-flow by CO<sub>2</sub> to check the influence of both total and partial replacement on the thermal field and the stability behaviors of the flames, and the other is to change the oxygen-diluent ratio in the coaxial-flow. The oxygen fraction in the oxidizer,  $\beta$ , is defined as:

$$\beta = \frac{Q(O_2)}{Q(O_2) + Q(Diluent)} \times 100\% \quad (1)$$

The pollutants emitted by the flames were measured by the probe sampling method, and two toxic gases of CO and NO<sub>x</sub> were considered. A thin quartz probe was axially mounted over the flame to extract exhaust products in the post-flame region. The quartz probe has a tapered tip with inner and outer diameters of 1 mm and 2 mm, respectively. Rapid pressure and temperature drop so occurred in the probe to quench chemical reactions and freeze the sample composition. The extracted sample gas firstly goes through a 1-m long stainless steel pipe for cooling down below 60 °C, and then enters two pollutant analyzers. One is NO/NO<sub>x</sub> analyzer (CLA, California Instruments Corporation, Model 400, San Diego, CA, USA) for NO<sub>x</sub> volumetric concentration, and the other is CO/CO<sub>2</sub> analyzer (NDIR, California Instruments Corporation, Model 300, San Diego, CA, USA) for CO and CO<sub>2</sub> volumetric concentrations. Before and after each measurement, zero and span calibrations were made to ensure reliable data are obtained. For all flames under testing, vertical traversing of the quartz probe showed that for a distance from 100 mm to 150 mm above the burner, the emission data obtained are rather constant. Hence, the distance of 110 mm was chosen for emission data comparison of the flames.

All measurements in this study were conducted several times and the averaged data were reported. An uncertainty analysis was made with the method suggested by Kline and McClintock [16]. Using a 95% confidence level, the uncertainties are 5.7% in flame temperature, 2.8% in flame lift height, 6.1% in CO volume concentration, 4.4% in CO<sub>2</sub> volume concentration, and 3.2% in NO<sub>x</sub> volume concentration.

### 3. Results and Discussions

#### 3.1. Flame Appearance

Although turbulent diffusion flames are more commonly seen in various practical applications, laminar diffusion flames are more attractive for researchers to understand the various phenomena such as flame extinction and pollutant formation. In this study, a laminar methane jet within a co-axially flowing oxidizer jet was discharged into a quiescent atmosphere. Typically, the flame would lift off the burner when the coaxial-flow velocity increases beyond a certain critical value, which is defined as threshold coaxial-flow velocity in current study, and the lifted flame will move farther downstream at a further higher coaxial-flow velocity. At sufficiently large coaxial-flow velocity, the lifted flame becomes unstable and blowout occurs. Furthermore, the flame extinguishes directly from an originally burner-attached flame is called blowoff. However, no blowoff was observed under the current

experimental conditions tested. In this study, the lift height was defined as the vertical distance from the nozzle exit to the lowest part of the visible flame base.

Table 1 shows the tested flow conditions where the methane flow rate was fixed at  $8.6 \times 10^{-6} \text{ m}^3/\text{s}$ . For such flows, the jet Froude number ( $Fr$ ) was calculated to be far below  $10^5$ , while the jet Reynolds number ( $Re$ ) was smaller than 2000, all indicating that the flows are within laminar regimes, and are thus buoyancy-dominated [17]. It was suggested that the triple flame position can be strongly affected by the stoichiometric laminar burning velocity. In this regards, the stoichiometric laminar burning velocity for methane at 1 atm and 298K was calculated from the 1D-Premixed code with detailed kinetic mechanism [18], with its value being 35 cm/s.

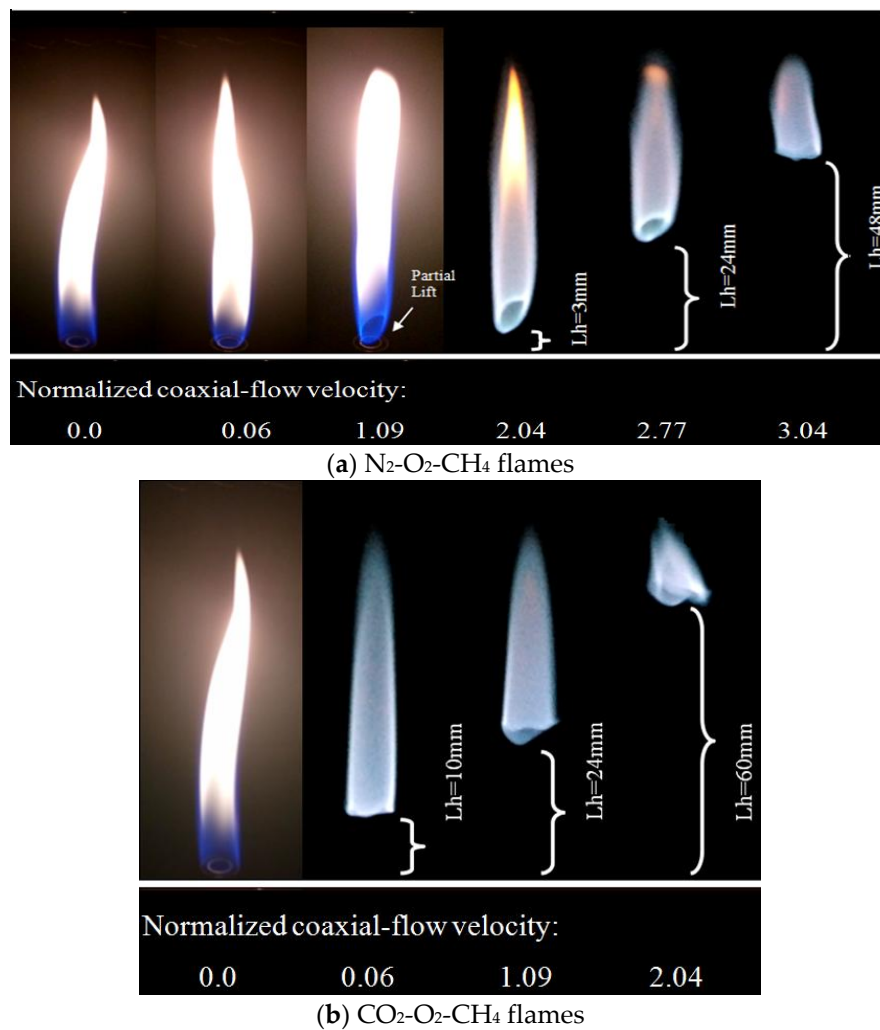
Flame photographs against increasing coaxial-flow velocity are given in Figure 2, with  $\text{N}_2$ -diluted flames shown in Figure 2a and  $\text{CO}_2$ -diluted flames shown in Figure 2b. It is obvious that both flames are attached to the burner rim at lower coaxial-flow velocity, while turn into detached at higher flow velocity. It is also observed that the flame lift height increases gradually with the increase in coaxial-flow velocity. For ease to inspect the relative strength of the flow speed and the mixture burning velocity, the coaxial-flow velocity is normalized by the stoichiometric burning velocity of 35 cm/s.

Figure 2a shows that as the normalized coaxial-flow velocity increases from  $Vn = 1.09$  to 2.04, the flame lifts off, and the lift height is  $Lh = 3 \text{ mm}$  at  $Vn = 2.04$ . Since the flame is lifted, the heat loss to the burner is minimized. Thus, it is expected that the combustion condition will change at the lifted flame base. This can be seen from the upper portion of the flame. At  $Vn = 1.09$ , the upper flame is much like those of the attached flames at  $Vn = 0.0$  and 0.06, being almost yellow indicative of soot formation in these flames. Once the flame is lifted, the region near to the lifted flame base changes its color from yellow to blue, indicating the occurrence of premixed combustion at the flame base. As the coaxial-flow velocity increases from  $Vn = 2.04$  to  $Vn = 2.77$ , the lift height further increases to  $Lh = 24 \text{ mm}$ . Meanwhile, the upper yellow soot-emitting region shrinks greatly, where only the yellow flame tip is noticeable. The lift height continues increasing to  $Lh = 48 \text{ mm}$  at  $Vn = 3.04$ , and finally, the flame blows out at  $Vn = 3.21$ .

In contrast, Figure 2b illustrates the flames where  $\text{N}_2$  is replaced by  $\text{CO}_2$ . First, the  $\text{CO}_2$ -diluted flame lifts at a much lower normalized coaxial-flow velocity of  $Vn = 0.06$  than  $Vn = 2.04$  for the  $\text{N}_2$ -diluted flame. Second, once lifted, the  $\text{CO}_2$ -diluted flame turns abruptly blue overall and maintains so for all other lifted flames at higher coaxial-flow velocity. Third, the  $\text{CO}_2$ -diluted flame blows off earlier, too, at  $Vn = 2.33$  in comparison to  $Vn = 3.21$  for the  $\text{N}_2$ -diluted flame. This means that there is a narrower operation range in terms of both attached and lifted stable flames after the co-flow composition is altered by replacing  $\text{N}_2$  by  $\text{CO}_2$ . Lastly, an apparent enlargement in the diameter of the lifted flame base is observable for the  $\text{CO}_2$ -diluted flame, while it is not very clear for the  $\text{N}_2$ -diluted flame.

For both flames, it is seen from the photos that as the lifted flame moves upwards, the luminous flame zone shortens, while the flame tip seems to be remained at a constant height. When approaching blowout, the surface of the flame, especially the flame base fluctuates vigorously. These fluctuating flames are prone to extinction and a further small increase in coaxial-flow velocity would lead to blowout. The constant flame tip height upon extinction that was observed in current work is similar to that reported in Ref. [19], in which a diffusion flame is lifted by an increasing fuel jet velocity, while it is caused by increasing coaxial-flow velocity in this study.

The physics for currently observed constant blowout position is assumed to be consistent with that of Moore et al. [20]. The authors proposed that the triple flame only exists within the flammable region, for instance, a region defined by two flammability limits of 5% and 15% mixture fraction contours, respectively. For the fixed fuel flow flame in this study, the flame height variation is minimized, despite a minor influence by the coaxial-flow. Due to rather constant flame height, the scalar field especially the mixture fraction contour corresponding to the lean flammability limit near the flame tip maintains in space, thus leading to blowout thereunto.



**Figure 2.** Flame photos against increasing coaxial-flow velocity at  $\beta = 21\%$ .

Figure 3 illustrates the flames when the oxygen fraction in the coaxial-flow is increased from that of air, namely 21% to 24%, and further to 27%. Figure 3a shows the photos of the  $\text{N}_2\text{-O}_2\text{-CH}_4$  flames under a constant coaxial-flow velocity of 0.38 m/s (normalized coaxial-flow velocity  $V_n = 1.09$ ). It is seen that as the oxygen fraction is increased higher than 21% in air, the otherwise partially-lifted flame gets attached to the burner nozzle. This is simply because the higher  $\text{O}_2$  concentration in the coaxial-flow mixture induces higher fuel burning velocity, and thus the flame front at the flame base propagates upstream towards the burner. Meanwhile, after reattachment is established, the blue flame in the region near the lifted flame base turns to a yellow soot-emitting region. Further increase in oxygen fraction from 24% to 27% does not have much influence on the soot-emitting region size, but the yellow color keeps changing brighter, which is indicative of intensified radiation.

In great contrast, the flames burning with the  $\text{CO}_2\text{-O}_2$  coaxial-flow, as shown in Figure 3b, display a color of totally blue with the oxygen fraction increasing from 21% to 27%. As known, the blue color indicative of no soot is linked to the low flame temperature in the  $\text{CO}_2$ -diluted flame in comparison with the  $\text{N}_2$ -diluted flame, the lower temperature of the  $\text{CO}_2$  flame is later discussed. In addition, the brightness is much weaker in comparison to the  $\text{N}_2$ -diluted flames. In fact, the presence of  $\text{CO}_2$  in the oxidizer has a much higher flow rate than the fuel flow rate, such that  $\text{CO}_2$  would act as a combustion inhibitor to hinder combustion chemical reactions. It is seen that the flame reattachment does not occur even at  $\beta = 27\%$  and it is thus expected to occur at further higher oxygen fraction.

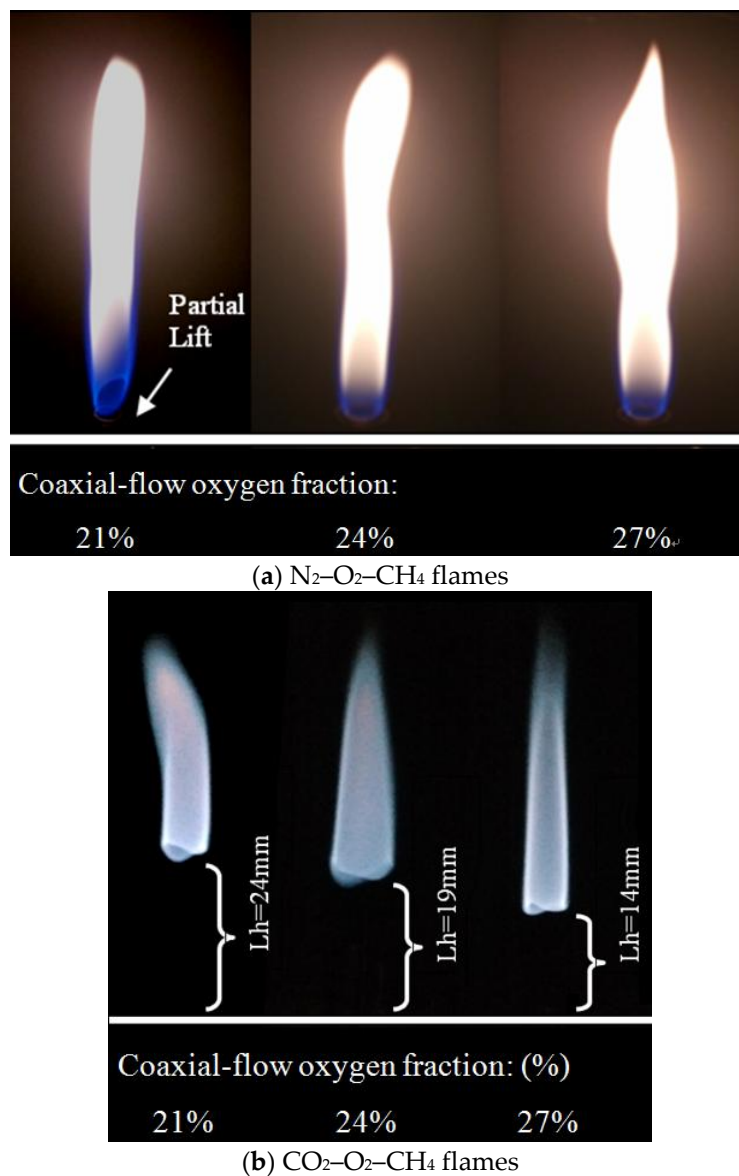


Figure 3. Flame photos against increasing oxygen fraction.

### 3.2. Flame Stability

Generally, for a diffusion flame of single fuel jet, if the jet velocity exceeds a critical value, then the flame base lifts off the burner and suspends at a certain distance above the burner. A further increase in jet velocity causes the liftoff height to increase until the lifted flame base approaches the flame tip at which point the flame blows out. The stabilization mechanism of a lifted flame is believed to be accomplished through the ‘triple flame’ [9–13]. It consists of rich premixed, diffusion, and lean premixed reaction zones that are attached at one point, which is called triple flame.

In the current study of co-axially double jet diffusion flame, similar behavior in flame liftoff and blowout is observed, as described in Section 3.1. From the experiments, it is found that when the annular coaxial-flow velocity exceeds a threshold value under constant central jet fuel flow, flame lift occurs. In this study, the threshold coaxial-flow velocity is obtained by gradually increasing the coaxial flow rate. According to the triple flame theory, the high coaxial-flow velocity destroyed the mixing between the fuel and oxidizer at the burner exit, and thus the flame tends to blow out or lift off due to the absence of flammable mixture [10]. To accurately locate this threshold value, the coaxial-flow

velocities were increased at a very small increment and only increasing flow rate are allowed to avoid the hysteresis coherent in flame liftoff process.

Figure 4 illustrates the flame lift behavior that was obtained within a coaxial-flow velocity range from 0.02 m/s to 1.49 m/s (normalized coaxial-flow velocity  $Vn = 0.06\sim 4.26$ ). From the figure, both the threshold value of coaxial-flow velocity for liftoff start and the relationship between lift height and coaxial-flow velocity are observable. For example, at the oxygen fraction of 21%, the  $N_2$ - $O_2$ - $CH_4$  flame lifts at the normalized velocity of  $Vn = 2.04$ , while the threshold coaxial-flow velocity for lifting the  $CO_2$ - $O_2$ - $CH_4$  flame at  $\beta = 21\%$  is much lower at  $Vn = 0.47$ . This indicates that the coaxial-flow oxidizer containing  $CO_2$  has a much stronger destabilizing effect on the central fuel jet flame. The reason for it is as follows. Firstly, the heat capacity of  $CO_2$ , by volume, is 1.67 times as much as that of  $N_2$ . The replacement of  $N_2$  by  $CO_2$  in the coaxial-flow increased the heat loss of the flame root. Together with the heat loss from the flame root to the burner rim, the  $CO_2$ -diluted flame is quenched so much that it lifts earlier than the  $N_2$ -diluted flame. In other words, the attached central flame can stand a much higher coaxial-flow velocity for  $N_2$ - $O_2$  composition than the  $CO_2$ - $O_2$  composition.

Similar phenomena appear for the two oxidizers at the oxygen fraction of 24%. As seen, the  $N_2$ - $O_2$  coaxial-flow lifts the flame at the normalized coaxial-flow velocity of  $Vn = 3.36$ , while the  $CO_2$ - $O_2$  mixture lifts the flame at a much lower value of around  $Vn = 0.60$ . At the oxygen fraction of 27%, due to an enhanced flame temperature that was caused by oxygen enrichment, no lifted  $N_2$ - $O_2$ - $CH_4$  flames are observed and the liftoff is expected to occur beyond the upper limit of the velocity range tested. In contrast, for the  $CO_2$ - $O_2$ - $CH_4$  flame, liftoff still occurs as the heat loss is still so much to quench the flame root. Guo et al. [21] also reported that the major influence of coaxial-flow on the lifted flame stabilization is through dilution effect, and thus the difference in the flame lifting behavior that is observed in this study can be ascribed to the thermal and chemical effects between the diluents of  $CO_2$  and  $N_2$ . Firstly,  $CO_2$  has larger specific heat than  $N_2$  and will induce a larger reduction in flame temperature and laminar burning velocity. Secondly,  $CO_2$  participates in chemical reactions and will slow down the forwards reaction rate from combustion reactants to products. That is, besides the thermal effect,  $CO_2$  also has chemical effect. Consequently, the difference in both the thermal and chemical effects between  $CO_2$  and  $N_2$  leads to the distinct threshold values of coaxial-flow velocity for flame liftoff start over.

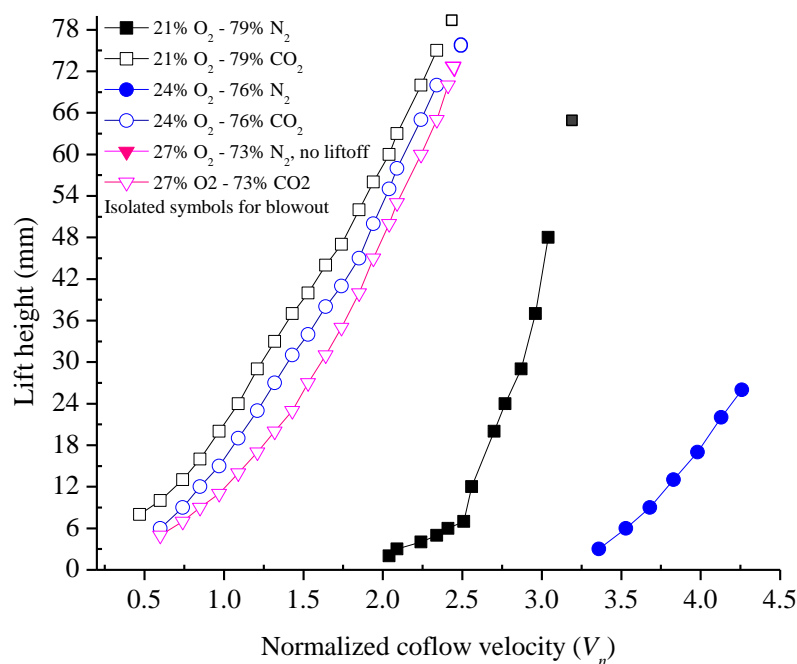


Figure 4. Flame lift height versus normalized coaxial-flow velocity.

Figure 4 also shows that as the oxygen level in the coaxial-flow oxidizer is enriched, i.e., from  $\beta = 21\%$  to  $24\%$ , the threshold coaxial-flow velocity for lifting the  $N_2$ -diluted flame increases from  $Vn = 2.04$  to  $Vn = 3.36$ , and at  $\beta = 27\%$  the threshold value (not shown in the figure) is beyond the upper limit of  $Vn = 4.26$ . In contrast, the threshold coaxial-flow velocity for the  $CO_2$ -diluted flame is increased to a much lesser extent, from  $Vn = 0.47$  at  $\beta = 21\%$  to  $Vn = 0.60$  at  $\beta = 27\%$ . In other words, the enhancement in flame stability due to oxygen enrichment is much more significant for the  $N_2$ - $O_2$ - $CH_4$  flame than the  $CO_2$ - $O_2$ - $CH_4$  flame. This reveals that the adoption of oxygen enrichment is a much effective method to enhance the stability of the  $N_2$ -diluted flames, but its effect is only marginal for the  $CO_2$ -diluted flames.

Figure 4 further points out that once the flame is lifted, the lift height increases with increasing coaxial-flow velocity. If excluding the initial phase of flame lifting where the lift height is only several millimeters, generally a linear increase in flame lift height with coaxial-flow velocity is observed. This linearly increasing lift height for the current co-axial jet flame is much similar to that of a single jet diffusion flame, which is reported by Ref. [19], that the lift height is proportional to the fuel jet velocity. At the initial phase of flame lifting, many factors tend to affect the lifting process, including local strain rate, heat loss to the nozzle, and exit velocity non-uniformity. Hence, usually partially lifted flames occur. However, when the flame is totally lifted off the burner rim, the triple flame theory supposed that the triple flame has a characteristic propagation speed and is stabilized where the propagation speed matches the local flow speed [10].

It is well known that carbon dioxide has a more significant reduction effect on laminar burning velocity than nitrogen. Therefore, at the same coaxial-flow velocity, due to the lower burning velocity of the  $CO_2$ - $O_2$ - $CH_4$  mixture, the triple flame stabilizing the lifted flame moves to a further downstream position when compared to the  $N_2$ - $O_2$ - $CH_4$  flame. The research [22] also proposed that the stably lifting flame is more dependent on the laminar burning velocity. Therefore, the lift height would behave in a much similar way as a premixed flame height. Namely, both heights are inversely proportional to the fuel reactivity, which can be characterized by laminar burning velocity.

On the other hand, it is seen from Figure 4 that for either  $N_2$ -diluted or  $CO_2$ -diluted flames under constant coaxial-flow velocity, the lift height is smaller at higher coaxial-flow oxygen fraction. The reason is also due to that the laminar burning velocity and fuel reactivity are increased at higher oxygen fraction, and thus the lifted flame move closer to the burner.

### 3.3. Flame Temperature

Due to the inter-diffusion of heat and mass between the fuel flow and oxidizer in the coaxial-flow and/or ambient air, flame centerline temperature is usually used to represent the state of fuel/oxidizer mixing and combustion for normal or inverse diffusion flame [23]. By traversing the thermocouple along the flame axis, the axial distributions of temperature was obtained and is shown in Figure 5 for both  $N_2$ -and  $CO_2$ -diluted flame at the oxygen fraction of  $\beta = 21\%$ . It is well known that for a single fuel jet diffusion flame, the flame centerline temperature is low in the potential core, increases in the transition region where fuel/air mixing as well as combustion develops, and finally achieves a maximum in the developed region. After that, the flame temperature drops in the post-flame region due to combustion decay and excessive entrained ambient cold air.

Figure 5 shows that at the very small velocity of coaxial-flow at  $Vn = 0.47$ , the axial distribution of flame centerline temperature should be similar to that of a single jet diffusion flame. Thereunto, the lowest temperature is  $800\text{ }^\circ\text{C}$  occurring at  $10\text{ mm}$  above the burner exit, indicating that the potential core height is no bigger than  $10\text{ mm}$ . As the coaxial-flow velocity increases, the potential core would be lengthened due to stretch that is caused by the coaxial-flowing annular jet. As a result, the flame centerline temperature at low elevations decreases. When the coaxial-flow velocity increases beyond the threshold value of  $Vn = 2.04$ , the  $N_2$ -diluted flame lifts off, and thus the temperature in the region between the burner exit and the lifted flame base would turn to room temperature of around  $21\text{ }^\circ\text{C}$ , as shown by the profiles of  $Vn = 2.77$  and  $Vn = 3.04$  in Figure 5. For both the attached and lifted flames,

the maximum centerline temperatures coincide in nearly the same elevation of 70 mm, confirming the afore-observation that these flames have similar flame tip height. Beyond the visible flame tip, the flame temperature drops and the data are omitted for clarity in Figure 5.

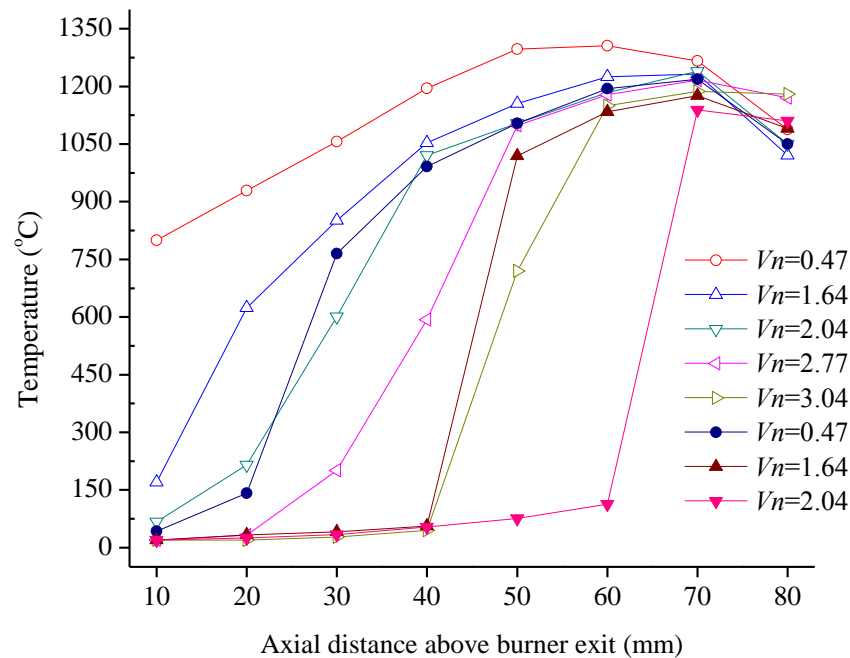


**Figure 5.** Axial distribution of flame centerline temperature for 21%O<sub>2</sub>–79%N<sub>2</sub> (open symbols) and 21%O<sub>2</sub>–79%CO<sub>2</sub> (solid symbols).

The CO<sub>2</sub>-diluted flames exhibit similar behavior in terms of the centerline flame temperature variation versus increasing coaxial-flow velocity. The difference is that even at the very small velocity of coaxial-flow at  $Vn = 0.47$ , the CO<sub>2</sub>-O<sub>2</sub>-CH<sub>4</sub> flame lifts, leading to low temperature upstream the flame base. A comparison with the N<sub>2</sub>-diluted flames reveals that under identical flow conditions, both the visible flame length and high-temperature flame zone are smaller for the CO<sub>2</sub>-diluted flames, which results in different pollutant emission behavior, which is to be discussed in next section.

### 3.4. Pollutants Emission

Based on probe sampling, pollutants measurements were conducted to obtain the volumetric concentrations of NO<sub>x</sub>, CO and CO<sub>2</sub> over the flame tip. Emission data for all flames at a fixed position 110 mm above the burner were reported. The reasons for using such raw data are threefold. First, for a laminar flame with low turbulence, the pollutant concentration in the flue gas typically has an exponential decay versus axial distance above the flame tip [24]. Second, the constant flame heights of various flames tend to give a constant flame tip position, due to the fixed fuel flow rate that was used. Third, the emission data at axial position is less influenced by ambient air than radial position. As a result of the three reasons, the axial position 110 mm above the flame tip that corresponds to the flat part of the exponential concentration curve was used to directly compare the various flames.

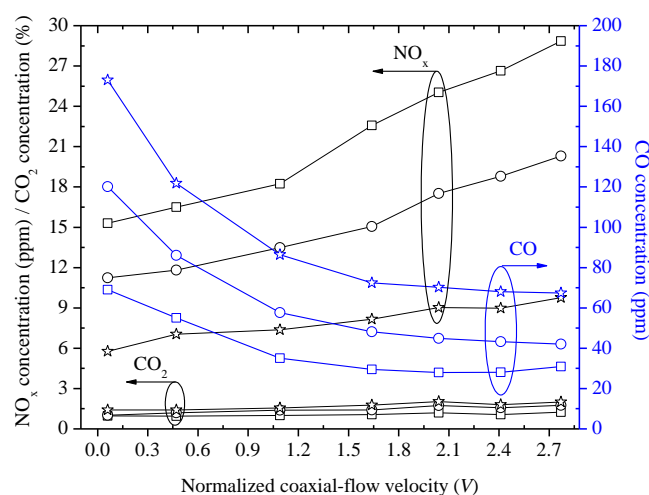
Experimental tests were firstly performed to inspect the emission variation with an increasing coaxial-flow rate, and then the emission was examined by varying the oxygen fraction in the coaxial-flow mixture. It is easily known that for the complete combustion of the supplied methane in the central jet, which is kept constant at  $8.6 \times 10^{-6} \text{ m}^3/\text{s}$  corresponding to a mean flow velocity of 0.22 m/s in this study, the flow rate of oxygen in the coaxial-flow required should be  $17.2 \times 10^{-6} \text{ m}^3/\text{s}$  so that the overall equivalence ratio equals one. However, due to stability restriction, for most of the flow conditions in Table 1, the supplied oxygen amount is below this stoichiometric value. It means that

in most flames tested, an overall fuel rich combustion occurs. It is expected that when the coaxial-flow rate increases, there is more oxygen supplied, thus leading the overall equivalence ratio towards one.

The temperature data in Section 3.3 revealed that the centerline flame temperature is below 1300 °C. Even though the temperature may be higher at the interface between the central fuel and the coaxial-flow and in the flame front region contacting the ambient air, such high temperature zones are quite thin and relatively small when compared to the inner flame zones [25]. Generally, the temperature below 1300 °C cannot activate the chain reactions in the Zeldovich mechanism [26]. Therefore, the possible NO formation for the current flames is by the Fenimore mechanism. The reason is that for atmospheric non-premixed flames, the Zeldovich and Fenimore mechanisms are considered to be controlling NO<sub>x</sub> emissions for a fuel with no bound nitrogen [26].

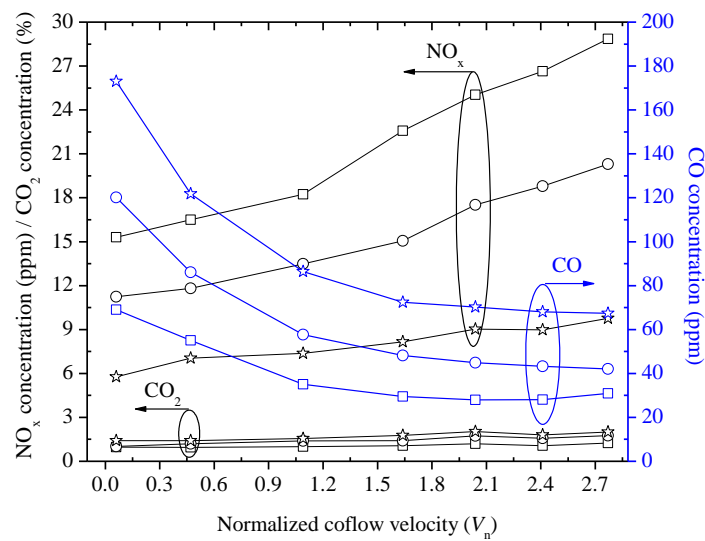
Figure 6 shows that for the N<sub>2</sub>-O<sub>2</sub> coaxial-flow with increasing velocity, the NO<sub>x</sub> concentration monotonically increases, while the CO concentration monotonically decreases. Further, the variation trends are the same at all oxygen fractions of  $\beta = 21\%$ , 24% and 27%. It is clear from Table 1 that for the present co-axial double jets, the overall equivalence ratio is below one. When the coaxial-flow velocity increases, there is more supplied oxygen in the annular jet to react with the central fuel, leading the overall equivalence ratio towards one. So, there would be more premixed or partially premixed combustion occurring within the flame. Additionally, the lifting process further promotes the transition from diffusion combustion to premixed combustion [19]. The enhanced premixed combustion can be seen from Figure 2 where the attached yellow flame shifts to lifted flames which are blue overall. Theoretically, blue color is due to the presence of CH radicals produced from pyrolysis of the fuel. Consequently, the developed premixed combustion generates plenty of CH radicals, which initiate NO formation via the Fenimore mechanism.

Figure 6 also shows that the CO concentration has a decreasing trend versus increasing coaxial-flow velocity. Firstly, it confirms that NO<sub>x</sub> and CO emissions are generally varying in opposite directions [27]. Secondly, the O<sub>2</sub> level in the coaxial-flow increases at higher coaxial-flow velocity, so the NO formation rate is accelerated, and meanwhile the conversion rate of CO into CO<sub>2</sub> is promoted, resulting in reduced CO emission. As for CO<sub>2</sub> emission, the figure shows that the CO<sub>2</sub> concentrations are mildly increasing with coaxial-flow velocity, due to more CO being converted into CO<sub>2</sub> at higher coaxial-flow velocity. Therefore, it is concluded that the concentrations of both CO and CO<sub>2</sub> are in opposite direction of NO<sub>x</sub> for the N<sub>2</sub>-diluted flame, i.e., the N<sub>2</sub>-O<sub>2</sub> coaxial-flow. Note that the unit for CO<sub>2</sub> concentrations is percentage in Figure 6.



(a)

Figure 6. Cont.



(b)

**Figure 6.**  $\text{NO}_x/\text{CO}_2/\text{CO}$  emissions versus  $\text{N}_2\text{-O}_2$  coaxial-flow velocity ( $\star$ :  $\beta = 21\%$ ;  $\circ$ :  $\beta = 24\%$ ;  $\square$ :  $\beta = 27\%$ ).

Comparison of pollutants concentrations at identical coaxial-flow velocity, but different oxygen fractions in Figure 6 reveals that the  $\text{NO}_x$  concentration increases while the CO concentration decreases when the oxygen fraction changes from 21% to 24% and further to 27%. At higher oxygen fraction, there are more  $\text{O}_2$  and O radical available in the flame on the one hand, and on the other, the enriched oxygen level enhances the fuel pyrolysis process to produce more CH radical. Both would result in a higher NO production rate, because O and CH radicals are the primary precursors for the Fenimore NO formation [28]. In addition, the enriched oxygen induces more intensive combustion, which can be seen from the more heavily illuminating flames in Figure 3 at  $\beta = 24\%$  and further  $\beta = 27\%$ . Thus, the contribution of thermal NO formation to the overall NO emission would also increase. Overall, there is higher  $\text{NO}_x$  concentration at higher oxygen fraction. On the contrary to  $\text{NO}_x$  emission, the higher temperature together with oxygen enriched environment accelerates the oxidation rate of CO [29]. As a result, the CO concentration is lower at a higher oxygen fraction.

When the  $\text{N}_2$  gas in the  $\text{N}_2\text{-O}_2$  coaxial-flow is totally replaced by  $\text{CO}_2$ , the emissions of  $\text{NO}_x/\text{CO}/\text{CO}_2$  are given in Figure 7. In great contrast to Figure 6, the  $\text{NO}_x$  concentrations decrease, while the CO concentrations increase against coaxial-flow velocity. First, the heat capacity of  $\text{CO}_2$  is larger than that of  $\text{N}_2$ . Thus, the replacement of  $\text{N}_2$  by  $\text{CO}_2$  directly leads to lower flame temperature as  $\text{CO}_2$  absorbs more heat than  $\text{N}_2$ . Second,  $\text{CO}_2$  is a very good fire/flame resistor, and its presence in the coaxial-flow behaves as a combustion inhibitor, separating the central fuel from ambient air and thus its component  $\text{N}_2$ . The  $\text{CO}_2$  in the coaxial-flow prohibits the contact between the fuel and ambient air ( $\text{N}_2$ ), and thus reducing NO formation. Consequently, the  $\text{NO}_x$  concentrations drop at higher coaxial-flow velocity where a larger part of the combustion zone will be enveloped by the increased amount of inhibitor gas  $\text{CO}_2$ . For the  $\text{CO}_2\text{-O}_2$  coaxial-flow flame, it is also true that a better mixing between the central fuel and annular oxidizer takes place at higher coaxial-flow velocity, which promotes premixed combustion, especially when the flame is lifted. However, the mixing between the two co-axial jets involves both  $\text{O}_2$  and  $\text{CO}_2$ , which are the components of the coaxial-flow. Albeit the  $\text{O}_2$  concentration in the coaxial-flow is increased, the  $\text{CO}_2$  in the coaxial-flow lowers the flame temperature by absorbing heat released by the combustion. Further, the amount of  $\text{CO}_2$  is dominant in the coaxial-flow, being more than both  $\text{O}_2$  and the fuel. Therefore, the flame temperature is actually reduced. The reduction in temperature can be seen in Figure 5, and hence the conversion rate of CO into  $\text{CO}_2$  is lowered,

leading to higher CO concentrations at higher coaxial-flow velocity. Figure 7 also indicates that the CO<sub>2</sub> concentration increases. This is simply due to the increased supply of CO<sub>2</sub> in the coaxial-flow.

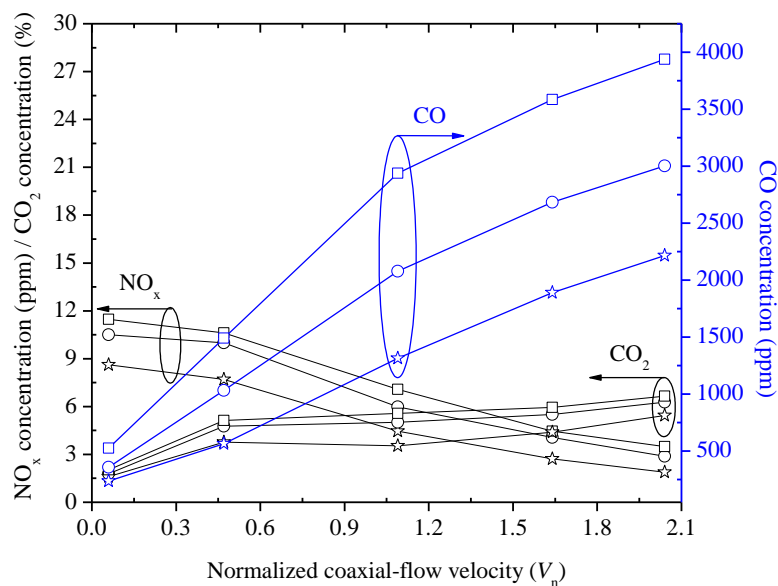


**Figure 7.** NO<sub>x</sub>/CO<sub>2</sub>/CO emissions versus CO<sub>2</sub>-O<sub>2</sub> coaxial-flow velocity (☆:  $\beta = 21\%$ ; O:  $\beta = 24\%$ ; □:  $\beta = 27\%$ ).

When a comparison is made of the CO and NO<sub>x</sub> concentrations at identical coaxial-flow velocity, but different oxygen fractions, Figure 7 shows that both CO and NO<sub>x</sub> emissions have an increase trend with increasing oxygen fraction within the coaxial-flow. When the oxygen level in the CO<sub>2</sub>-O<sub>2</sub> mixture becomes higher, the combustion condition is improved as more oxygen is supplied to draw the overall equivalence ratio towards one. Hence, the fuel will be burned more completely by the increased oxygen supply, the heat release will be enhanced [30], and in the meantime, the combustion products, including CO and NO<sub>x</sub>, also increase.

The partial replacement of N<sub>2</sub> in the coaxial-flow by CO<sub>2</sub> is also tested and the resultant emission behavior is shown in Figure 8. In this case, a fifty percent of N<sub>2</sub> in the original N<sub>2</sub>-O<sub>2</sub> coaxial-flow has been replaced by CO<sub>2</sub>, resulting in a coaxial-flow composition involving three gases of N<sub>2</sub>, CO<sub>2</sub>, and O<sub>2</sub>. Figure 8 shows that for such partial replacement, the pollutants emission characteristic is much similar to the case of total replacement. Specifically, as the coaxial-flow velocity increases, the NO<sub>x</sub> concentration decreases while the CO concentration increases. This can be ascribed to the same reason similar to the total replacement case in Figure 7. That is, the N<sub>2</sub>-CO<sub>2</sub>-O<sub>2</sub> mixture exhibits an overall flame-inhibiting behavior similar to that of the CO<sub>2</sub>-O<sub>2</sub> mixture. As the coaxial-flow velocity increases, the annular jet enveloping the central fuel develops in strength and cuts off the contact between the fuel and ambient O<sub>2</sub> and N<sub>2</sub> in air. Although there is direct N<sub>2</sub> present in the coaxial-flow, the NO formation rate is lower in comparison to the baseline case, i.e., the N<sub>2</sub>-O<sub>2</sub> mixture. First, the effect of partial replacement of N<sub>2</sub> by CO<sub>2</sub> is that the otherwise high Fenimore NO production rate between the fuel and N<sub>2</sub> in the N<sub>2</sub>-O<sub>2</sub> coaxial-flow would decay due to the reduced concentration of N<sub>2</sub>. Second, in comparison to the ambient air composition of N<sub>2</sub>-O<sub>2</sub>, the coaxial-flow composition of N<sub>2</sub>-CO<sub>2</sub>-O<sub>2</sub> would act as a flame resistor due to its high CO<sub>2</sub> concentration. Therefore, as a result of suppressed combustion, the NO<sub>x</sub> concentration shows a decrease trend at higher coaxial-flow velocity. Simultaneously, the combustion becomes less complete, leading the CO concentration to increase, which resembles the case of total N<sub>2</sub> replacement by CO<sub>2</sub> in Figure 7.

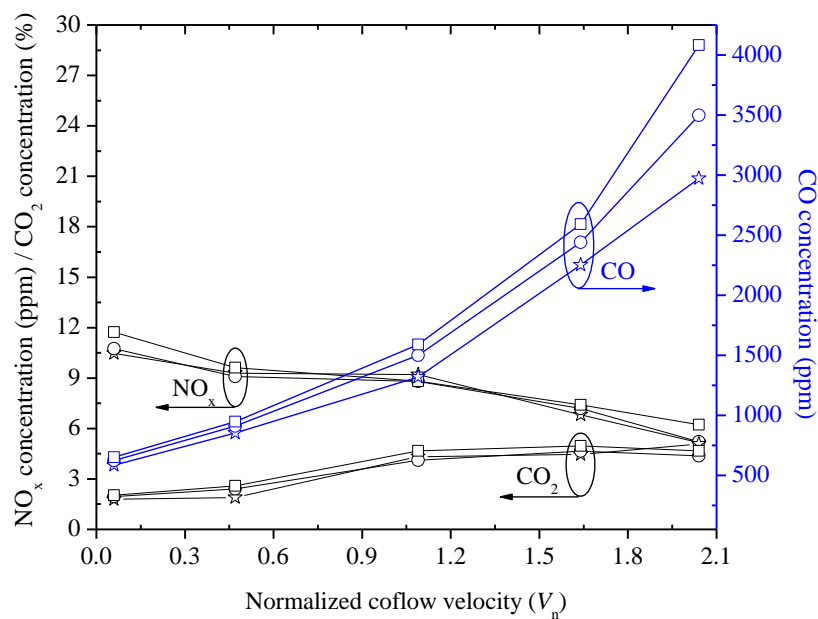


**Figure 8.** NO<sub>x</sub>/CO<sub>2</sub>/CO emissions versus N<sub>2</sub>-CO<sub>2</sub>-O<sub>2</sub> coaxial-flow velocity (☆:  $\beta = 21\%$ ; O:  $\beta = 24\%$ ; □:  $\beta = 27\%$ ).

It is of interest to compare both NO<sub>x</sub> and CO emissions for the flames that are burning with different coaxial-flow compositions. For the base case, i.e., the N<sub>2</sub>-O<sub>2</sub> mixture, Figure 6 shows that in the coaxial-flow range of  $V_n = 0.06\text{--}4.26$ , the NO<sub>x</sub> concentration curves peak at the highest  $V_n = 2.77$  with the maximum value of 28.8 ppm. When N<sub>2</sub> is replaced or partially replaced by CO<sub>2</sub>, Figures 7 and 8 indicate that the maximum NO<sub>x</sub> concentrations are no higher than 11.5 ppm. The reduction in NO<sub>x</sub> emission has two reasons. One is that the CO<sub>2</sub> replacement of N<sub>2</sub> tends to lower flame temperature, which in return minimizes the possibilities of thermal NO formation. The other reason is that the CO<sub>2</sub> introduced in the flames participates in chemical reactions, thus competing CH with the Fenimore NO mechanism, which also consumes CH radical, through the reaction  $\text{CO}_2 + \text{CH} \rightarrow \text{HCO} + \text{CO}$  [31]. As for CO emission, its concentrations in Figure 6 for baseline case are no higher than 173 ppm. Figures 7 and 8 show that the maximum CO concentration after total or partial replacement is 4083 ppm, even the lowest value is above 236 ppm. This reveals that there is a surge in the CO emission once N<sub>2</sub> is totally or partially replaced by CO<sub>2</sub>. This is consistent with the fact that more CO is produced under a CO<sub>2</sub>-rich environment, through the reaction  $\text{CO}_2 + \text{H} \rightarrow \text{CO} + \text{OH}$  [31].

#### 4. Conclusions

Total and partial replacement of N<sub>2</sub> by CO<sub>2</sub> in the coaxial-flow oxidizer has been experimentally conducted to examine the resultant change in flame stability, thermal, and emission characteristics. A double concentric burner was adopted to operate the flame in the lifted regime. Methane was used as the fuel in the central jet and the annular jet comprising the N<sub>2</sub>-O<sub>2</sub>, CO<sub>2</sub>-O<sub>2</sub>, or N<sub>2</sub>-CO<sub>2</sub>-O<sub>2</sub> mixtures was used as the coaxial-flowing oxidizer. Experiments were performed at fixed fuel flow rate, while increasing the coaxial-flow rate, and meanwhile the oxygen-diluent ratio is adjusted from 21% to 27%.

The data report a critical coaxial-flow velocity, beyond which the diffusion flame lifts off the burner, and a linear increase in lift height with coaxial-flow velocity for both N<sub>2</sub>-diluted and CO<sub>2</sub>-diluted flames. The lifted flames always blew out towards a constant flame tip height, which is intimately related to the constant flame height/fuel flow rate used. Replacement of N<sub>2</sub> in the coaxial-flow by CO<sub>2</sub> greatly reduced the threshold coaxial-flow velocity for liftoff, indicating deteriorated flame stability. When the oxygen fraction in the coaxial-flow increases, the threshold coaxial-flow velocity increases.

This increase is more significant for the N<sub>2</sub>-diluted flame, due to the stronger detrimental effect of CO<sub>2</sub> on combustion.

The centerline temperatures of both N<sub>2</sub>- and CO<sub>2</sub>-diluted flames are low and are generally below 1300 °C, making the thermal NO production negligible in comparison to the prompt NO production. Besides, NO and CO emissions are found to be highly dependent on the coaxial-flow composition and velocity. With increasing velocity of the N<sub>2</sub>-O<sub>2</sub> coaxial-flow, NO<sub>x</sub> emissions monotonically increase, while CO emissions monotonically decrease. When N<sub>2</sub> in the N<sub>2</sub>-O<sub>2</sub> oxidizer is replaced or partially replaced by CO<sub>2</sub>, NO<sub>x</sub> emissions reversed its direction to monotonically drop at higher coaxial-flow velocity, due to the strong flame-resisting behavior of CO<sub>2</sub>. For all cases, CO emissions are observed to vary in the opposite direction of NO<sub>x</sub> emissions. Replacement also leads the NO<sub>x</sub> emissions to be lowered, while the CO emissions to be heavily increased.

**Author Contributions:** Haisheng Zhen conceived and designed the experiments, performed the experiments and analyzed the data; The other two authors contributed reagents/materials/analysis tools.

**Acknowledgments:** This study was supported by National Natural Science Foundation of China (51766003).

**Conflicts of Interest:** The authors declare no conflict of interest.

## Nomenclature

<i>Fr</i>	jet Froude number
<i>Re</i>	jet Reynolds number
$\Phi$	overall equivalence ratio
<i>Q</i>	volumetric flow rate, m <sup>3</sup> /s
$\beta$	oxygen fraction in co-flow, %
<i>V<sub>n</sub></i>	normalized co-flow velocity
<i>L<sub>h</sub></i>	flame lift off height, mm

## References

1. Wall, T.; Liu, Y.H.; Spero, C.; Elliott, L.; Khare, S.; Rathnam, R.; Zeenathal, F.; Moghtaderi, B.; Buhre, B.; Sheng, C.D.; et al. An overview on oxyfuel coal combustion-state of the art research and technology development. *Chem. Eng. Res. Des.* **2009**, *87*, 1003–1006. [[CrossRef](#)]
2. Toftegaard, M.B.; Brix, J.; Jensen, P.A.; Glarborg, P.; Jensen, A.D. Oxy-fuel combustion of solid fuels. *Prog. Energy Combust. Sci.* **2010**, *36*, 581–625. [[CrossRef](#)]
3. Horn, F.L.; Steinberg, M. Control of carbon dioxide emissions from a power plant (and use in enhanced oil recovery). *Fuel* **1982**, *61*, 415–422. [[CrossRef](#)]
4. Andersson, K.; Johnsson, F. Flame and radiation characteristics of gas-fired O<sub>2</sub>/CO<sub>2</sub> combustion. *Fuel* **2007**, *86*, 656–668. [[CrossRef](#)]
5. Liu, F.; Guo, H.; Smallwood, G.J. The chemical effect of CO<sub>2</sub> replacement of N<sub>2</sub> in air on the burning velocity of CH<sub>4</sub> and H<sub>2</sub> premixed flames. *Combust. Flame* **2003**, *133*, 495–497. [[CrossRef](#)]
6. Heil, P.; Toporov, D.; Förster, M.; Kneer, R. Experimental investigation on the effect of O<sub>2</sub> and CO<sub>2</sub> on burning rates during oxyfuel combustion of methane. *Proc. Combust. Inst.* **2011**, *33*, 3407–3413. [[CrossRef](#)]
7. Glarborg, P.; Bentzen, L.L.B. Chemical effects of a high CO<sub>2</sub> concentration in oxy-fuel combustion of methane. *Energy Fuels* **2008**, *22*, 291–296. [[CrossRef](#)]
8. Watanabe, H.; Marumo, T.; Okazaki, K. Effect of CO<sub>2</sub> reactivity on NO<sub>x</sub> formation and reduction mechanisms in O<sub>2</sub>/CO<sub>2</sub> combustion. *Energy Fuel* **2012**, *26*, 938–951. [[CrossRef](#)]
9. Phillips, H. Flame in a buoyant methane layer. *Symp. (Int.) Combust.* **1965**, *10*, 1277–1283. [[CrossRef](#)]
10. Wu, C.Y.; Chao, Y.C.; Cheng, T.S.; Li, Y.H.; Lee, K.Y.; Yuan, T. The blowout mechanism of turbulent jet diffusion flames. *Combust. Flame* **2006**, *145*, 481–494. [[CrossRef](#)]
11. Lee, W.J.; Park, J.; Kwon, O.B.; Yoon, J.H.; Keel, S.I. Heat-loss-induced self-excitation in laminar lifted coflow-jet flames. *Proc. Combust. Inst.* **2015**, *35*, 1007–1014. [[CrossRef](#)]

12. Wang, Q.; Hu, L.H.; Zhang, M.; Tang, F.; Zhang, X.C.; Lu, S.X. Lift-off of jet diffusion flame in sub-atmospheric pressures: An experimental investigation and interpretation based on laminar flame speed. *Combust. Flame* **2014**, *161*, 1125–1130. [[CrossRef](#)]
13. Jeon, M.K.; Kim, N.I. Direct estimation of edge flame speeds of lifted laminar jet flames and a modified stabilization mechanism. *Combust. Flame* **2017**, *186*, 140–149. [[CrossRef](#)]
14. Kalghatgi, G.T. Blow-out stability of gaseous jet diffusion flames. Part I: In still air. *Combust. Sci. Technol.* **1981**, *26*, 233–239. [[CrossRef](#)]
15. Blevins, L.G.; Pitts, W.M. Modeling of bare and aspirated thermocouples in compartment fires. *Fire Saf. J.* **1999**, *33*, 239–259. [[CrossRef](#)]
16. Kline, S.J.; McClintock, F.A. Describing uncertainties in single sample experiments. *Mech. Eng.* **1953**, *75*, 3–8.
17. Peters, N.; Gottgens, J. Scaling of buoyant turbulent jet diffusion flames. *Combust. Flame* **1990**, *85*, 206–214. [[CrossRef](#)]
18. Wei, Z.L.; Leung, C.W.; Cheung, C.S.; Huang, Z.H. Single-valued prediction of markers on heat release rate for laminar premixed biogas-hydrogen and methane-hydrogen flames. *Fuel* **2017**, *133*, 35–45. [[CrossRef](#)]
19. Kiran, D.Y.; Mishra, D.P. Experimental studies of flame stability and emission characteristics of simple LPG jet diffusion flame. *Fuel* **2007**, *86*, 1545–1551. [[CrossRef](#)]
20. Moore, N.J.; McCraw, J.L.; Lyons, K.M. Observations on jet-flame blowout. *Int. J. React. Syst.* **2008**, *2008*, 1–7. [[CrossRef](#)]
21. Guo, H.S.; Min, J.S.; Galizzié, C.; Escudi, D.; Baillet, F. A numerical study on the effects of CO<sub>2</sub>/N<sub>2</sub>/Ar addition to air on liftoff of a laminar CH<sub>4</sub>/air diffusion flame. *Combust. Sci. Technol.* **2010**, *182*, 1549–1563. [[CrossRef](#)]
22. Lawn, C.J. Lifted flames on fuel jets in co-flowing air. *Prog. Energy Combust. Sci.* **2009**, *35*, 1–30. [[CrossRef](#)]
23. Dong, L.L.; Cheung, C.S.; Leung, C.W. Combustion optimization of a port-array inverse diffusion flame jet. *Energy* **2011**, *36*, 2834–2846. [[CrossRef](#)]
24. Sze, L.K.; Cheung, C.S.; Leung, C.W. Appearance, temperature, and NO<sub>x</sub> emission of two inverse diffusion flames with different port design. *Combust. Flame* **2006**, *144*, 237–248. [[CrossRef](#)]
25. Sara, M.A.; Chen, J.Y.; Fernandez-Pello, A.C. *Fundamentals of Combustion Processes*; Springer Science & Business Media: Berlin, Germany, 2011; pp. 139–142.
26. Turns, S.R. Understanding NO<sub>x</sub> formation in nonpremixed flames: Experiments and modeling. *Prog. Energy Combust. Sci.* **1995**, *21*, 361–385. [[CrossRef](#)]
27. Syred, N.; Chigier, N.A.; Beer, J.M. Flame stabilization in recirculation zones of jets with swirl. *Proc. Combust. Inst.* **1971**, *13*, 617–624. [[CrossRef](#)]
28. Briones, A.M.; Som, S.; Aggarwal, S. Effect of multistage combustion on NO<sub>x</sub> emissions in methane-air flames. *Combust. Flame* **2007**, *149*, 448–462. [[CrossRef](#)]
29. Zhen, H.S.; Miao, J.; Leung, C.W.; Cheung, C.S.; Huang, Z.H. A study on the effects of air preheat on the combustion and heat transfer characteristics of Bunsen flames. *Fuel* **2016**, *184*, 50–58. [[CrossRef](#)]
30. Li, J.; Huang, H.Y.; Li, H.H.T.; Osaka, Y.; Bai, Y.; Kobayashi, N. Combustion and heat release characteristics of biogas under hydrogen- and oxygen-enriched condition. *Energies* **2017**, *10*, 1200. [[CrossRef](#)]
31. Oh, J.; Noh, D. The effect of CO<sub>2</sub> addition on the flame behavior of a non-premixed oxy-methane jet in a lab-scale furnace. *Fuel* **2014**, *117*, 79–86. [[CrossRef](#)]

